Molecular Pharmacology Fast Forward. Published on November 8, 2013 as DOI: 10.1124/mol.113.089581
This article has not been copyedited and formatted. The final version may differ from this version.
Molecular Pharmacology Fast Forward. Published on November 8, 2013 as doi:10.1124/mol.113.089581

Title Page.

Cross modulation and molecular interaction at the $Ca_v3.3$ protein between the endogenous lipids and the T-type calcium channel antagonist TTA-A2.

Magali Cazade, Cindy E. Nuss, Isabelle Bidaud, John J. Renger, Victor N. Uebele, Philippe Lory and Jean Chemin.

Institut de Génomique Fonctionnelle, Universités Montpellier 1 & 2, Centre National de la Recherche Scientifique (CNRS) Unité Mixte de Recherche (UMR) 5203, INSERM U661, LabEx 'Ion Channel Science and Therapeutics', Montpellier, F34094 France.

M.C., I.B., P.L. & J.C.

Department of Neuroscience, Merck Research Laboratories, West Point, USA.

C.E.N., J.J.R. & V.N.U.

Downloaded from molpharm.aspetjournals.org at ASPET Journals on April 9, 2024

Copyright 2013 by the American Society for Pharmacology and Experimental Therapeutics.

Molecular Pharmacology Fast Forward. Published on November 8, 2013 as DOI: 10.1124/mol.113.089581
This article has not been copyedited and formatted. The final version may differ from this version.

Running Title Page.

Lipids and TTA-A2 interaction at the $Ca_v3.3$ protein

Corresponding Author: Jean Chemin or Philippe Lory,

Jean Chemin, Institut de Génomique Fonctionnelle, Universités Montpellier 1 & 2, Centre National de la Recherche Scientifique (CNRS), Unité Mixte de Recherche (UMR) 5203, INSERM U661, LabEx 'Ion Channel Science and Therapeutics', 141, rue de la Cardonille, 34094 Montpellier cedex 05, France.

Phone: +33 4 34 35 92 50 / Fax: +33 4 67 54 24 32 / Email : jean.chemin@igf.cnrs.fr

Philippe Lory, Institut de Génomique Fonctionnelle, Universités Montpellier 1 & 2, Centre National de la Recherche Scientifique (CNRS), Unité Mixte de Recherche (UMR) 5203, INSERM U661, LabEx 'Ion Channel Science and Therapeutics', 141, rue de la Cardonille, 34094 Montpellier cedex 05, France.

Phone: +33 4 34 35 92 51 / Fax: +33 4 67 54 24 32 / Email : philippe.lory@igf.cnrs.fr

Number of text pages: 32

Number of tables: 0

Number of figures: 5

Number of References: 46

Number of words in Abstract: 237

Number of words in Introduction: 437

Number of words in Discussion: 1513

Downloaded from molpharm.aspetjournals.org at ASPET Journals on April 9, 2024

Molecular Pharmacology Fast Forward. Published on November 8, 2013 as DOI: 10.1124/mol.113.089581
This article has not been copyedited and formatted. The final version may differ from this version.

Non-standard abbreviations:

T-channel: T-type calcium channel; *N*AGly: *N*-arachidonoyl glycine; *N*AGABA-OH: *N*-arachidonoyl-3-OH-gaba-butyric acid; *N*AGABA: *N*-arachidonoyl-gaba-butyric acid; *N*ASer: *N*-arachidonoyl-L-serine; *N*AAla: *N*-arachidonoyl alanine; *N*ATau: *N*-arachidonoyl taurine; *N*A-5HT: *N*-arachidonoyl serotonin; *N*ADA: *N*-arachidonoyl dopamine; *N*AEA: *N*-arachidonoyl ethanolamine (anandamide); 22:6 Gly: *N*-docosahexaenoyl glycine; 20:0 Gly: *N*-arachidoyl glycine; 18:2 Gly: *N*-linoleoyl glycine; TTA-A1: (R)-2-(4-(tert-butyl)phenyl)-N-(1-(5-methoxypyridin-2-yl)ethyl)acetamide; TTA-A2: (R)-2-(4-cyclopropylphenyl)-N-(1-(5-(2,2,2-trifluoroethoxy)pyridin-2-yl)ethyl)acetamide; TTA-Q4: (S)-4-(6-chloro-4-cyclopropyl-3-(2,2-difluoroethyl)-2-oxo-1,2,3,4-tetrahydroquinazolin-4-yl)benzonitrile.

Downloaded from molpharm.aspetjournals.org at ASPET Journals on April 9, 2024

Abstract.

T-type calcium channels (T/Ca_v3 channels) are implicated in various physiological and patho-physiological processes such as epilepsy, sleep disorders, hypertension and cancer. T-channels are the target of endogenous signaling lipids including the endocannabinoid anandamide, the ω3-fatty acids and the lipoamino-acids. However, the precise molecular mechanism by which these molecules inhibit T-current is unknown. In this study we provided a detailed electrophysiological and pharmacological analysis indicating that the effects of the major *N*-acyl derivatives on the Ca_v3.3 current share many similarities with those of TTA-A2, a synthetic T-channel inhibitor. Using radioactive binding assays with the TTA-A2 derivative [^{3}H]-TTA-A1, we demonstrated that poly-unsaturated lipids which inhibit the Ca_v3.3 current, as *N*AGly, *N*ASer, anandamide, *N*ADA, *N*ATau and *N*A-5HT, all displaced [^{3}H]-TTA-A1 binding to membranes prepared from cells expressing Ca_v3.3, with K_i in a micromolar or sub-micromolar range. In contrast, lipids with a saturated alkyl chain, as *N*-arachidoyl glycine and *N*-arachidoyl ethanolamine, which did not inhibit the Ca_v3.3 current, had no effect on [^{3}H]-TTA-A1 binding. Accordingly, bio-active lipids occluded TTA-A2 effect on Ca_v3.3 current. In addition, TTA-Q4, a positive allosteric modulator of [^{3}H]-TTA-A1 binding and TTA-A2 functional inhibition, acted in a synergistic manner to increase lipid-induced inhibition of the Ca_v3.3 current. Overall, our results demonstrate a common molecular mechanism for the synthetic T-channel inhibitors and the endogenous lipids, and indicate that TTA-A2 and TTA-Q4 could be important pharmacological tools to dissect the involvement of T-current in the physiological effects of endogenous lipids.

Downloaded from molpharm.aspetjournals.org at ASPET Journals on April 9, 2024

Molecular Pharmacology Fast Forward. Published on November 8, 2013 as DOI: 10.1124/mol.113.089581
This article has not been copyedited and formatted. The final version may differ from this version.

Introduction.

Low-voltage-activated (T-type / Ca_v3) calcium channels are a subclass of voltage-dependent calcium channels allowing calcium entry near the resting potential of most cells (Perez-Reyes, 2003). T-channels are implicated in many physiological processes as diverse as neuronal firing (Cain and Snutch, 2010; Perez-Reyes, 2003), slow wave sleep (Lee and Shin, 2007), hormone secretion (Weiss and Zamponi, 2012), cell cycle (Lory et al., 2006), heart rhythm (Ono and Iijima, 2010) and vasodilatation (Kuo et al., 2011). They emerge as important pharmacological targets in several diseases such as epilepsy, insomnia, neuropathic pain, cancer and hypertension (McGivern, 2006; Todorovic and Jevtovic-Todorovic, 2013).

Various synthetic T-channel blockers have been described in the past few years (Giordanetto et al., 2011; Lory and Chemin, 2007; McGivern, 2006), including TTA-A2, a potent and specific inhibitor of T-current (Kraus et al., 2010; Reger et al., 2011; Uebele et al., 2009a; Uebele et al., 2009b). *In-vivo* studies demonstrated that TTA-A2 reduces absence epilepsy seizures (Reger et al., 2011; Uebele et al., 2009b), pain perception (Francois et al., 2013), nicotine self administration (Uslaner et al., 2010), weight gain (Uebele et al., 2009a) whereas it ameliorates the sleep quality (Kraus et al., 2010; Reger et al., 2011; Uebele et al., 2009a) and displays anti-psychotic properties (Uslaner et al., 2012).

T-channels are also inhibited by several endogenous signaling lipids. These molecules include arachidonic acid, ω3-fatty acids, endocannabinoids (as anandamide), lipoamino-acids and lipo-neurotransmitters (Barbara et al., 2009; Chemin et al., 2001; Chemin et al., 2007; Danthi et al., 2005; Gilmore et al., 2012; Ross et al., 2009; Talavera et al., 2004; Zhang et al., 2000). These lipids are implicated in multiple physiological functions and more specifically in pain perception (Basbaum et al., 2009; Bradshaw and Walker, 2005; Burstein, 2008), sleep and epilepsy (Chen and Bazan, 2005), heart rhythm and vasodilatation (Leaf et al., 2003; Roman, 2002).

Downloaded from molpharm.aspetjournals.org at ASPET Journals on April 9, 2024

Molecular Pharmacology Fast Forward. Published on November 8, 2013 as DOI: 10.1124/mol.113.089581
This article has not been copyedited and formatted. The final version may differ from this version.

Lipid-mediated inhibition of T-current occurred in excised cell-free membrane patches consistent with direct effect of lipids on T-channels or via perturbation of their near membrane environment (Barbara et al., 2009; Chemin et al., 2001; Chemin et al., 2007; Talavera et al., 2004). In this context, it is interesting to note that a radiolabeled derivative of TTA-A2, [^{3}H]-TTA-A1, was shown to bind membranes from cells expressing $Ca_v3.3$ with a Kd of 1.8 nM (Uebele et al., 2009b). Moreover a structurally distinct antagonist, TTA-Q4, increased both [^{3}H]-TTA-A1 binding and TTA-A2-induced inhibition of the $Ca_v3.3$ current, by acting on a distinct molecular site of the $Ca_v3.3$ protein (Uebele et al., 2009b). In this study, we used these new pharmacological tools to explore whether bio-active lipids and TTA-A2 share similar mechanisms and molecular determinants at the $Ca_v3.3$ protein.

Downloaded from molpharm.aspetjournals.org at ASPET Journals on April 9, 2024

Molecular Pharmacology Fast Forward. Published on November 8, 2013 as DOI: 10.1124/mol.113.089581
This article has not been copyedited and formatted. The final version may differ from this version.

Materials and Methods.

Cell culture and transfection protocols.

tsA-201 cells and a HEK-293 cell line stably expressing $Ca_v3.3$ (a generous gift from Dr. Perez-Reyes (Xie et al., 2007)) were cultivated in DMEM supplemented with GlutaMax and 10% fetal bovine serum (Invitrogen). tsA-201 cell transfection was performed using jet-PEI (QBiogen) with a DNA mix containing 0.5% of a GFP plasmid and 99.5% of either of the plasmid constructs that code for human $Ca_v3.1a$, $Ca_v3.2$, and $Ca_v3.3$. Two days after transfection, cells were dissociated with Versene (Invitrogen) and plated at a density of ~35 x 10^3 cells per 35 mm Petri dish for electrophysiological recordings.

Electrophysiological recordings.

Macroscopic currents were recorded in the whole cell configuration using an Axopatch 200B amplifier (Molecular Devices). The extracellular solution contained the following (in mM): 135 NaCl, 20 TEACl, 2 $CaCl_2$, 1 $MgCl_2$, and 10 HEPES (pH adjusted to 7.25 with KOH,~330 mOsm). Borosilicate glass pipettes have a typical resistance of 1.5–2.5 MΩ when filled with an internal solution containing the following (in mM): 140 CsCl, 10 EGTA, 10 HEPES, 3 Mg-ATP, 0.6 GTPNa, and 3 $CaCl_2$ (pH adjusted to 7.25 with KOH, ~315 mOsm). In a subset of experiments, EGTA was substituted with 10 mM BAPTA. Recordings were performed at room temperature and were filtered at 2–5 kHz. Data were analyzed using pCLAMP9 (Molecular Devices) and GraphPad Prism (GraphPad) software. Drugs were applied by a gravity-driven homemade perfusion device and control experiments were performed using the solvent alone. Results are presented as the mean ± SEM, and n is the number of cells used. Student' t test were used to compare the different values, which were considered significant at $p<0.05$.

Binding Experiments.

Downloaded from molpharm.aspetjournals.org at ASPET Journals on April 9, 2024

Molecular Pharmacology Fast Forward. Published on November 8, 2013 as DOI: 10.1124/mol.113.089581
This article has not been copyedited and formatted. The final version may differ from this version.

Membranes were prepared from the HEK 293 cells stably expressing $Ca_v3.3$ (Uebele et al., 2009b). Protein concentration was determined using the Bio-Rad protein assay (Bio-Rad, Hercules, CA, USA). Binding assays were performed at room temperature for 3 h with 8 µg protein, 1 nM [^{3}H]-TTA-A1 and increasing concentrations of lipids (ranging from 1 nM to 40 µM) in 1 ml final volume in Packard Unifilter-96, GF/C plates (Packard, Meriden, CT, USA) coated with 0.3% ethylene imine polymer solution (Sigma-Aldrich). Assay and wash buffer contained 20 mM HEPES, 125 mM NaCl, and 5 mM KCl. After incubation, the reactions were aspirated and washed with 4°C buffer using a Perkin-Elmer 96-well Filtermate Harvester. The plates were dried before the addition of Microscint-20 (Perkin-Elmer Life and Analytic Sciences, Shelton, CT, USA) and the remaining radioactivity was quantified on a Perkin-Elmer NXT HTS Top Count. Total and non-specific binding were determined in the absence and the presence of 100 nM of TTA-A2, respectively. Data were collected in triplicate. The inhibition constants K_i were calculated with GraphPad Prism using the following equation: $K_i = IC_{50} / (1+([[^3H]\text{-TTA-A1}]/Kd))$ where IC_{50} was the half maximal inhibitory concentration, [[^{3}H]-TTA-A1] was 1 nM and Kd was 1.8 nM, as previously described (Uebele et al., 2009b).

Chemical reagents.

[^{3}H]-TTA-A1 (56–65 mCi/mmol), TTA-A2 and TTA-Q4 were synthesized at Merck (West Point, PA), as previously described (Uebele et al., 2009b), dissolved in DMSO at 10 mM, aliquoted and kept at -20°C. Lipids were obtained from Cayman Chemical and were dissolved in ethanol purged with argon at a concentration of 10 mM. *N*A-5HT and *N*ADA were also obtained from Tocris Bioscience and Enzo Life Sciences, and the results were similar using lipids from different suppliers. Stock lipid solutions were briefly sonicated, aliquoted, sealed

Downloaded from molpharm.aspetjournals.org at ASPET Journals on April 9, 2024

Molecular Pharmacology Fast Forward. Published on November 8, 2013 as DOI: 10.1124/mol.113.089581
This article has not been copyedited and formatted. The final version may differ from this version.

under argon, and kept at -80°C. These aliquots were dissolved daily in the extracellular solution. Control experiments were performed using the solvent alone.

Downloaded from molpharm.aspetjournals.org at ASPET Journals on April 9, 2024

Molecular Pharmacology Fast Forward. Published on November 8, 2013 as DOI: 10.1124/mol.113.089581
This article has not been copyedited and formatted. The final version may differ from this version.

Results.

Inhibition of $Ca_v3.3$ currents by poly-unsaturated amino-acids.

We have characterized the effects of lipoamino-acids on the $Ca_v3.3$ current because among lipids inhibiting T-currents, only this class showed a higher T-type specificity, with no effect on cannabinoid receptors and TRPV1 (Barbara et al., 2009; Bradshaw and Walker, 2005; Huang et al., 2001). We found that the $Ca_v3.3$ current was strongly inhibited by 3 µM *N*-docosahexaenoyl glycine (chain length 22 carbons, 6 doubles bonds, 22:6 Gly) at a holding potential (HP) of -75 mV (Fig. 1A) but not at HP -110 mV (Fig. 1B). The inhibition occurred in the minute range and was relieved by application of 3 mg/ml bovine serum albumin (Barbara et al., 2009; Gilmore et al., 2012)(BSA, Fig. 1C). The extent of inhibition increased gradually with the number of double bonds in the *N*-acyl glycine (Fig. 1E). The saturated *N*-arachidoyl glycine (20:0 Gly) produced weak inhibition (~13 %, n=5, Fig. 1D-E), *N*-linoleoyl glycine (18:2 Gly) produced ~50 % inhibition (n=7, Fig. 1E, $p \leq 0.001$ compared to 20:0 Gly), *N*-arachidonoyl glycine (20:4, *N*AGly) produced ~67 % inhibition (n=11, Fig. 1E, $p \leq 0.05$ compared to 18:2 Gly) and the fully poly-unsaturated 22:6 glycine produced ~74 % inhibition (n=12, Fig. 1E, non-significant compared to 20:4 Gly). Interestingly, the increase in the number of double bonds in fatty acids augments the membrane fluidity whereas it restricts the conformational freedom of the molecule possibly leading to the adequate conformation to inhibit T-current. The $Ca_v3.3$ current was also inhibited by several *N*-arachidonoyl amino-acids including *N*-arachidonoyl-3-OH-γ-butyric acid (*N*AGABA-OH, ~81 % inhibition (n=22)), *N*-arachidonoyl-γ-butyric acid (*N*AGABA, ~59 % inhibition (n=24)), *N*-arachidonoyl-L-serine (*N*ASer, ~64 % inhibition (n=22)) and *N*-arachidonoyl alanine (*N*AAla, ~45 % inhibition (n=23, Fig. 1E)). In addition, the lipo-neurotransmitters *N*-arachidonoyl taurine (*N*ATau), *N*-arachidonoyl serotonin (*N*A-5HT) and *N*-arachidonoyl dopamine (*N*ADA) inhibited the $Ca_v3.3$ current by ~74 %, ~34 % and ~20 %, respectively (Fig. 1E,

Downloaded from molpharm.aspetjournals.org at ASPET Journals on April 9, 2024

Molecular Pharmacology Fast Forward. Published on November 8, 2013 as DOI: 10.1124/mol.113.089581
This article has not been copyedited and formatted. The final version may differ from this version.

n≥8). Similar findings were obtained with *N*ADA and *N*A-5HT using an intracellular medium containing 10 mM BAPTA (n=5) (Gilmore et al., 2012; Ross et al., 2009) as well as on $Ca_v3.1$ and $Ca_v3.2$ current (data not shown). Application of 3 µM *N*ADA induced ~18 % inhibition of the $Ca_v3.1$ current (n=5) and ~27 % inhibition of the $Ca_v3.2$ current (n=6). Similarly, application of 3 µM *N*A-5HT induced ~44 % inhibition of the $Ca_v3.1$ current (n=16) and ~50 % inhibition of the $Ca_v3.2$ current (n=14). As previously described (Chemin et al., 2001), in these experiments, 3 µM *N*AEA strongly inhibited the three Ca_v3 currents by ~74-80 % (n≥8, Fig. 1E).

NAGly effect on $Ca_v3.3$ biophysical properties.

*N*AGly inhibited the $Ca_v3.3$ current at every potential with inhibition of the peak current at -35 mV by ~40 % with 1 µM *N*AGly and by ~70 % with 3 µM *N*AGly (Fig. 2A). *N*AGly had weak and not significant effect on the $Ca_v3.3$ current-voltage relationship since the $V_{0.5}$ values were -45.7 ± 1.3 mV (n=8) in control condition, -49.6 ± 1.4 mV (n=8) during 1 µM *N*AGly application and -48.6 ± 0.8 mV (n=5) during 3 µM *N*AGly application ($p>0.05$). We also observed that 3 µM *N*AGly accelerated the inactivation rate of $Ca_v3.3$ current at every tested potential ($p<0.05$, n=5, Fig. 2B) without significant corresponding effect on the activation rate (Fig. 2C). Furthermore, *N*AGly induced a ~10 mV negative shift in the steady-state inactivation properties of $Ca_v3.3$ (Fig. 2D). The $V_{0.5}$ values were -73.1 ± 0.9 mV (n=8) in control condition, -80.6 ± 1.07 mV ($p<0.001$, n=8) during 1 µM *N*AGly application and -83.2 ± 0.8 mV ($p<0.001$, n=7) during 3 µM *N*AGly application. Application of 3 µM *N*AGly also decreased the slope factor of the steady-state inactivation curve of $Ca_v3.3$ from 5.2 ± 0.2 in control condition to 4.3 ± 0.2 ($p<0.05$). We next investigated the effect of *N*AGly on the recovery from inactivation of $Ca_v3.3$ current (Fig. 2E). The recovery from inactivation of $Ca_v3.3$ current was well fit by a mono-exponential revealing that *N*AGly strongly increased

Downloaded from molpharm.aspetjournals.org at ASPET Journals on April 9, 2024

Molecular Pharmacology Fast Forward. Published on November 8, 2013 as DOI: 10.1124/mol.113.089581
This article has not been copyedited and formatted. The final version may differ from this version.

the τ of recovery from 298 ± 20 ms (n=8) in control condition to 453 ± 22 ms (p<0.001, n=8) during 1 µM *N*AGly application and to 771 ± 43 ms (p<0.001, n=8) during 3 µM *N*AGly application. Finally, we found that both 1 µM and 3 µM *N*AGly slowed the deactivation of the $Ca_v3.3$ current at repolarization potentials ranging from -120 to -60 mV (p<0.05, n=8, Fig. 2F).

Pharmacological interaction of endogenous lipids and TTA-A2 on the $Ca_v3.3$ channel.

Recently, TTA-A2, a potent and specific synthetic inhibitor of T-current was described (Kraus et al., 2010; Reger et al., 2011; Uebele et al., 2009a; Uebele et al., 2009b). As observed with endogenous lipids, TTA-A2 inhibited the Ca_v3 current at physiological HP but not at very negative potentials (i.e. -110 mV) (Francois et al., 2013; Kraus et al., 2010). Furthermore, as observed with endogenous lipids, TTA-A2 induced a negative shift in the steady-state inactivation properties of Ca_v3 current and slowed their recovery from inactivation (Francois et al., 2013; Kraus et al., 2010). It should be noted that several other structurally-unrelated T-channel inhibitors, including mibefradil, flunarizine and pimozide, which also exhibit similar state-dependent inhibition of T-currents (Martin et al., 2000; Santi et al., 2002), were shown to interact with [^{3}H]-TTA-A1 binding to membranes containing $Ca_v3.3$ (Uebele et al., 2009b). Therefore we investigated whether endogenous lipids and TTA-A2 could share a common inhibitory mechanism on $Ca_v3.3$. To this purpose, the effect of *N*AEA (which strongly inhibited $Ca_v3.3$ current) and *N*ADA or *N*A-5HT (which mildly inhibited $Ca_v3.3$ current) were compared in the presence and the absence of TTA-A2 (Fig. 3). We found that 300 nM *N*AEA alone induced 56 ± 2 % inhibition of the $Ca_v3.3$ current and accelerated the inactivation kinetic (τ) by 32.5 ± 2.6 % (p<0.05, n=8; Fig. 3A), as previously described (Chemin et al., 2001). Similarly, 3 nM TTA-A2 alone induced 52 ± 3 % inhibition of the $Ca_v3.3$ current but slowed the inactivation kinetic (τ) by 34.1 ± 5.4 % (p<0.05, n=7;

Downloaded from molpharm.aspetjournals.org at ASPET Journals on April 9, 2024

Molecular Pharmacology Fast Forward. Published on November 8, 2013 as DOI: 10.1124/mol.113.089581
This article has not been copyedited and formatted. The final version may differ from this version.

Fig. 3B). Interestingly, when *N*AEA and TTA-A2 were applied simultaneously, the $Ca_v3.3$ current was inhibited by 70 ± 2 % (n=10; Fig. 3C), indicating that the effect of *N*AEA and TTA-A2 are only partially additive (Fig. 3G). In this latter case, the inactivation kinetic (τ) was accelerated by 21.7 ± 4.9 % ($p<0.05$, n=10; Fig. 3C). The results were not different ($p>0.05$) when both molecules were applied after *N*AEA application (n=5, Fig. 3A) or TTA-A2 application (n=5, Fig. 3B). These results were further confirmed using the mild inhibitors *N*ADA and *N*A-5HT. Indeed, when 3 µM *N*A-5HT, which inhibited the $Ca_v3.3$ current by 20 ± 4 % (n=16; Fig. 3D), was applied with TTA-A2, the resulting inhibition was only 33 ± 4 % (n=19; Fig. 3F) demonstrating no additive effects. This was clearly evidenced when *N*A-5HT and TTA-A2 where applied together after TTA-A2 treatment (Fig. 3E). In this case the inhibition induced by both compounds was less than those obtained with TTA-A2 alone ($p<0.01$, n=11, Fig. 3E and Fig. 3G). Similar findings were obtained with 3 µM *N*ADA (n=15, Fig. 3G). Overall, these results demonstrated a pharmacological interaction between endogenous lipids and TTA-A2 and suggested that both molecules could share the same molecular site on the $Ca_v3.3$ protein.

N-acyl derivatives that inhibited $Ca_v3.3$ current displaced [^{3}H]-TTA-A1 binding.

Because lipids and TTA-A2 possibly act at the same molecular site, we investigated whether bio-active lipids that inhibit $Ca_v3.3$ current could displace [^{3}H]-TTA-A1 (a radiolabeled derivative of TTA-A2) binding to membranes containing $Ca_v3.3$, as demonstrated for several state-dependent T-channel antagonists (Uebele et al., 2009b). We found that *N*-arachidonoyl amino-acids *N*ASer and *N*AGly, which inhibited $Ca_v3.3$ current (Fig. 1D), displaced [^{3}H]-TTA-A1 binding in a concentration–dependent manner (Fig. 4A). The K_i for *N*ASer was 9.02 ± 0.06 µM and 7.12 ± 0.31 µM for *N*AGly whereas the Hill slope number (n_{Hill}) was 2.1 and 1.8 for *N*ASer and *N*AGly, respectivelly. Displacement of [^{3}H]-

Downloaded from molpharm.aspetjournals.org at ASPET Journals on April 9, 2024

Molecular Pharmacology Fast Forward. Published on November 8, 2013 as DOI: 10.1124/mol.113.089581
This article has not been copyedited and formatted. The final version may differ from this version.

TTA-A1 binding was not observed with the saturated arachidoyl glycine at concentrations up to 40 μM (20:0, Fig. 4A). Similarly, the endocannabinoid anandamide (20:4 EA) displaced [^{3}H]-TTA-A1 binding with a K_i of 1.35 ± 0.04 μM and a n_{Hill} of 2.4, but not the saturated form, *N*-arachidoyl ethanolamine (Fig. 4B). In addition, the *N*-arachidonoyl neurotransmitters *N*ATau, *N*-arachidonoyl dopamine (*N*ADA) and *N*-arachidonoyl serotonin (*N*A-5HT), also displaced [^{3}H]-TTA-A1 binding (Fig. 4C). The K_i was 4.13 ± 0.11 μM for *N*ATau, 0.170 ± 0.004 μM for *N*ADA and 0.026 ± 0.001 μM for *N*A-5HT whereas the n_{Hill} was 1.5, 1.3 and 1.1 for *N*ATau, *N*ADA and *N*A-5HT, respectively.

TTA-Q4, a positive allosteric modulator of [^{3}H]-TTA-A1 binding, increased lipid-induced inhibition of Ca_v3.3 current.

The structurally distinct T-type antagonist, TTA-Q4, was shown to increase [^{3}H]-TTA-A1 binding on Ca_v3.3 expressing membranes as well as TTA-A2-induced Ca_v3.3 current inhibition (Uebele et al., 2009b). It was demonstrated that TTA-Q4 increased TTA-A2-mediated Ca_v3.3 current inhibition by a synergistic mechanism (Uebele et al., 2009b). Therefore, we investigated whether TTA-Q4 had a similar effect on lipid-induced Ca_v3.3 current inhibition. We found that 20 nM TTA-Q4 alone induced 22 ± 4 % inhibition of Ca_v3.3 current (n=8, Fig. 5A), 100 nM anandamide alone induced 18 ± 5 % inhibition (n=5, Fig. 5B) whereas application of both compounds induced 72 ± 4 % inhibition (n=7, Fig. 5C-D), which is much greater than the anticipated sum of ~40% expected for additive effects (as indicated by an arrow in Fig. 5I). We also found that 300 nM *N*A-5HT induced negligible effect on Ca_v3.3 current (8 ± 5 % inhibition, n=5, Fig. 5E) whereas when *N*A-5HT was applied with TTA-Q4, the inhibition of Ca_v3.3 current was 52 ± 2 % (n=5, Fig 5G-I). Similar results were obtained using 3 μM *N*ADA and 20 nM TTA-Q4 since application of both compounds

Downloaded from molpharm.aspetjournals.org at ASPET Journals on April 9, 2024

Molecular Pharmacology Fast Forward. Published on November 8, 2013 as DOI: 10.1124/mol.113.089581
This article has not been copyedited and formatted. The final version may differ from this version.

induced 72 ± 2 % inhibition of $Ca_v3.3$ current (n=11, Fig. 5I). Overall, these results indicated that TTA-Q4 and poly-unsaturated lipids modulated $Ca_v3.3$ current in a synergistic manner.

Downloaded from molpharm.aspetjournals.org at ASPET Journals on April 9, 2024

Molecular Pharmacology Fast Forward. Published on November 8, 2013 as DOI: 10.1124/mol.113.089581
This article has not been copyedited and formatted. The final version may differ from this version.

Discussion

In this study we demonstrated that lipid effects on $Ca_v3.3$ biophysical properties share many features with those induced by TTA-A2, especially regarding the "gating properties". Importantly, inhibition of $Ca_v3.3$ current by both lipids and TTA-A2 occurs only at depolarized resting potentials at which $Ca_v3.3$ channels are partly inactivated. We also documented that endogenous lipids and TTA-A2 share similar molecular mechanisms. Firstly, we found that TTA-A2 effects on $Ca_v3.3$ current were weakly additive with those produced by lipids or were even decreased when both lipids and TTA-A2 were applied together. Secondly, using [^{3}H]-TTA-A1, a radioactive derivative of TTA-A2, which specifically binds membranes expressing $Ca_v3.3$ (Uebele et al., 2009b), we found that endogenous lipids inhibiting $Ca_v3.3$, all displaced [^{3}H]-TTA-A1 binding with K_i in the micromolar range. Thirdly, using TTA-Q4, which increased [^{3}H]-TTA-A1 binding on $Ca_v3.3$ expressing membranes as well as TTA-A2-induced $Ca_v3.3$ current inhibition (Uebele et al., 2009b), we demonstrated a synergistic mechanism between this molecule and lipids for $Ca_v3.3$ current inhibition. Overall, our results indicate a common molecular mechanism between the synthetic inhibitor TTA-A2 and the endogenous lipids, and suggest that lipids inhibiting the T-current could act directly on the $Ca_v3.3$ protein at a site overlapping that of TTA-A2. However, we cannot exclude that lipids could displace [^{3}H]-TTA-A1 binding by acting at the membrane rather than on the $Ca_v3.3$ protein. Importantly, no [^{3}H]-TTA-A1 binding was observed in membrane from HEK-293 cells that did not express $Ca_v3.3$ (Uebele et al., 2009b).

We have shown that *N*-arachidonoyl derivatives containing a glycine, a serine, an alanine, a γ-butyric acid, a 3-OH-γ-butyric acid and a taurine inhibited the $Ca_v3.3$ current. Inhibition did not occur with the saturated *N*-arachidoyl glycine (20:0) and increased with the number of double bonds leading to maximal effect on $Ca_v3.3$ current with the fully poly-unsaturated ω3 *N*-docosahexaenoyl glycine (22:6 gly). Similar findings were obtained for

Downloaded from molpharm.aspetjournals.org at ASPET Journals on April 9, 2024

Molecular Pharmacology Fast Forward. Published on November 8, 2013 as DOI: 10.1124/mol.113.089581
This article has not been copyedited and formatted. The final version may differ from this version.

$Ca_v3.1$ and $Ca_v3.2$ currents (not shown), as previously observed with fatty acids and *N*-acyl ethanolamines (Chemin et al., 2007). In contrast with previous studies (Gilmore et al., 2012; Ross et al., 2009), we found that *N*A-5HT and *N*ADA were weak inhibitors of the $Ca_v3.3$ currents (as well as $Ca_v3.1$ and $Ca_v3.2$ currents). Similar results were obtained using a stable HEK-293 cell line expressing $Ca_v3.3$ current or using an intracellular medium containing 10 mM BAPTA (Gilmore et al., 2012; Ross et al., 2009). We do not have yet any satisfactory explanation for this discrepancy because the Ca_v3 subunits and the lipids used here are identical and from the same companies as those previously used (Gilmore et al., 2012; Ross et al., 2009). We also demonstrated that the inhibition occurred only at depolarized resting potentials indicating that lipids preferentially affect T-channels in the inactivated state or in intermediate closed states (Talavera et al., 2004). Furthermore, *N*AGly induced a hyperpolarized shift in the $Ca_v3.3$ steady-state inactivation properties leading to current inhibition at physiological resting potentials. In addition, we found that *N*AGly slowed the recovery from inactivation of $Ca_v3.3$ current, a property that was not investigated before on recombinant channels. These effects on inactivation properties were reminiscent of those induced by TTA-A2, which induced similar effects on steady-state inactivation and recovery from inactivation (Francois et al., 2013; Kraus et al., 2010). *N*AGly also induced a hyperpolarized shift in the steady-state inactivation of $Ca_v3.1$ and $Ca_v3.2$ currents and slowed their recovery from inactivation confirming a common biophysical mechanism (data not shown). However, *N*AGly had specific effects on the $Ca_v3.3$ current kinetics. *N*AGly accelerated the inactivation kinetics of $Ca_v3.3$ current at every tested potential without the corresponding effect on $Ca_v3.1$ and $Ca_v3.2$ currents (data not shown). In the same way, *N*AGly induced a deceleration of the $Ca_v3.3$ deactivation kinetic, which was not observed on $Ca_v3.1$ and $Ca_v3.2$ currents (data not shown) and is not yet documented for TTA-A2.

Downloaded from molpharm.aspetjournals.org at ASPET Journals on April 9, 2024

Molecular Pharmacology Fast Forward. Published on November 8, 2013 as DOI: 10.1124/mol.113.089581
This article has not been copyedited and formatted. The final version may differ from this version.

We found that TTA-A2 induced inhibition of $Ca_v3.3$ current was not fully additive with those produced by anandamide when both compounds were applied together. Moreover, the presence of *N*ADA or *N*A-5HT decreased the TTA-A2 effect, probably because they did not produce an important inhibition *per-se*, suggesting that they could share with TTA-A2 a common site on $Ca_v3.3$. This was confirmed using [^{3}H]-TTA-A1, a radioactive derivative of TTA-A2, which specifically binds membranes expressing $Ca_v3.3$ (Uebele et al., 2009b). Indeed, we demonstrated that poly-unsaturated lipids *N*AGly, *N*ASer, *N*AEA, *N*ADA, *N*A-5HT and *N*ATau, all displaced the [^{3}H]-TTA-A1 binding with K_i in a micromolar or sub-micromolar range whereas saturated lipids (which did not inhibit $Ca_v3.3$ current) had no effect. The affinity (K_i in µM) obtained with poly-unsaturated lipids were *N*A-5HT (0.02) < *N*ADA (0.17) < *N*AEA (1.35) < *N*ATau (4.13) < *N*AGly (7.12) < *N*ASer (9.02). These findings are in good agreement with our electrophysiological studies on $Ca_v3.3$ current inhibition. Interestingly, we also found that *N*ADA and *N*A-5HT, which had mild effect on $Ca_v3.3$ current, strongly bound to $Ca_v3.3$ expressing membranes. Accordingly, the presence of *N*ADA or *N*A-5HT prevented TTA-A2 inhibitory effects in electrophysiological experiments. We have previously shown that inhibitory effects of lipids on T-current depend on both the amide and the hydroxyl groups (Chemin et al., 2007). In this context, the aromatic heterocyclic rings of *N*ADA and *N*A-5HT, which increase the distance between the amide and the hydroxyl groups and are also hydrophobic, could impair interaction with key amino-acids in the $Ca_v3.3$ protein and therefore their inhibitory effect, without decreasing their binding to membranes expressing $Ca_v3.3$. This suggests that the poly-unsaturated alkyl chain of lipids would be mostly important for their binding whereas the amide and hydroxyl groups would mediate current inhibition. Accordingly, both *N*ADA and *N*A-5HT strongly occluded TTA-A2 effect but weakly inhibited $Ca_v3.3$ current whereas saturated lipids (which did not produce inhibition) provided no consistent displacement. We also found that the Hill slope number

Downloaded from molpharm.aspetjournals.org at ASPET Journals on April 9, 2024

Molecular Pharmacology Fast Forward. Published on November 8, 2013 as DOI: 10.1124/mol.113.089581
This article has not been copyedited and formatted. The final version may differ from this version.

(n_{Hill}) in these binding assays were high (ranged from 1.5 to 2.4) for *N*ATau, *N*AGly, *N*ASer and *N*AEA, especially for *N*AEA (n_{Hill} = 2.4), whereas the n_{Hill} for *N*A-5HT and *N*ADA were more typical of competitive displacement curves (n_{Hill} between 1.1 and 1.3). These result might indicate lipid degradation because in these binding experiments we did not use a fatty acid amide hydrolase (FAAH, the main enzyme metabolizing *N*AEA and others *N*Arachidonoyl-conjugates (Huang et al., 2001; Saghatelian et al., 2006; Saghatelian et al., 2004)) inhibitor and this enzyme is known to be very active even in crude membrane extracts (Childers et al., 1994; Deutsch and Chin, 1993; Pinto et al., 1994). For instance, displacement of the cannabinoid receptor CB1 agonist [^{3}H]-CP-55940 by *N*AEA, indicated K_i of 2 µM in the absence of the FAAH inhibitor PMSF whereas K_i was 12 nM in the presence of PMSF (Pinto et al., 1994), suggesting *N*AEA degradation. Interestingly, the same authors showed that the slope of the displacement curve was particularly steep (n_{Hill} > 2) in the absence of PMSF whereas in the presence of PMSF the n_{Hill} was near a value of 1 (Pinto et al., 1994). Interestingly, *N*A-5HT and *N*ADA are inhibitors of FAAH and particularly *N*A-5HT (Bisogno et al., 2000; Bisogno et al., 1998) and this FAAH inhibition could account for the strong *N*A-5HT potency in the binding assay. In addition, it is important to note that in these membrane extracts, the trans-membrane resting potential was likely lost, and the $Ca_v3.3$ channels might be in a complete inactivated state that was not achieved in electrophysiological experiments, and this could also explain the potency of *N*A-5HT and *N*ADA in these binding assays.

Because the structurally distinct antagonist, TTA-Q4, was shown to be a positive allosteric modulator of TTA-A2, increasing [^{3}H]-TTA-A1 binding on $Ca_v3.3$ expressing membranes as well as TTA-A2 induced $Ca_v3.3$ current inhibition (Uebele et al., 2009b), we have investigated whether it could also promote lipid-induced $Ca_v3.3$ current inhibition. We found that TTA-Q4 potentiated *N*AEA effect on $Ca_v3.3$ current, indicating that TTA-Q4 and anandamide could inhibit $Ca_v3.3$ current in a synergistic manner. Moreover, in the presence of

Downloaded from molpharm.aspetjournals.org at ASPET Journals on April 9, 2024

Molecular Pharmacology Fast Forward. Published on November 8, 2013 as DOI: 10.1124/mol.113.089581
This article has not been copyedited and formatted. The final version may differ from this version.

TTA-Q4 we revealed important *N*ADA and *N*A-5HT inhibitory effects, as previously described (Gilmore et al., 2012; Ross et al., 2009). Interestingly, the binding and the potency of anandamide at CB1 and TRPV1 receptors is increased by palmitoyl ethanolamine and oleoyl ethanolamine, which acts as an allosteric modulator of these receptors, a phenomenon called the “entourage” effect (Ben-Shabat et al., 1998; De Petrocellis et al., 2001; Ho et al., 2008).

It was demonstrated that TTA-A2 had important pharmacological effects including the reduction of absence epilepsy seizures (Reger et al., 2011; Uebele et al., 2009b) and of pain perception (Francois et al., 2013). In addition, TTA-A2 affected sleep/wake patterns (Kraus et al., 2010; Reger et al., 2011; Uebele et al., 2009a) and displayed anti-psychotic properties (Uslaner et al., 2012). Similarly, bio-active lipids inhibiting T-currents have been implicated in several functions, including pain perception (Basbaum et al., 2009; Bradshaw and Walker, 2005; Burstein, 2008), sleep and epilepsy (Chen and Bazan, 2005). The analogy between *in-vivo* effects of TTA-A2 and lipids, suggests, in the light of our results, that many physiological effects of endogenous lipids are supported by T-current inhibition. Furthermore, TTA-A2 and TTA-Q4 could be important pharmacological tools to dissect the involvement of T-current in the physiological effects of endogenous lipids.

Downloaded from molpharm.aspetjournals.org at ASPET Journals on April 9, 2024

Molecular Pharmacology Fast Forward. Published on November 8, 2013 as DOI: 10.1124/mol.113.089581
This article has not been copyedited and formatted. The final version may differ from this version.

Aknowledgments

We are very grateful to Drs T. Durroux and F. Rassendren for insightful discussions and critical reading of the manuscript.

Downloaded from molpharm.aspetjournals.org at ASPET Journals on April 9, 2024

Molecular Pharmacology Fast Forward. Published on November 8, 2013 as DOI: 10.1124/mol.113.089581
This article has not been copyedited and formatted. The final version may differ from this version.

Authorship Contributions

Participated in research design: Uebele, Lory and Chemin

Conducted experiments: Cazade, Nuss, Bidaud and Chemin

Contributed new reagents or analytic tools: Renger and Uebele

Performed data analysis: Uebele and Chemin

Wrote or contributed to the writing of the manuscript: Uebele, Lory and Chemin

Downloaded from molpharm.aspetjournals.org at ASPET Journals on April 9, 2024

Molecular Pharmacology Fast Forward. Published on November 8, 2013 as DOI: 10.1124/mol.113.089581
This article has not been copyedited and formatted. The final version may differ from this version.

References

Barbara G, Alloui A, Nargeot J, Lory P, Eschalier A, Bourinet E and Chemin J (2009) T-type calcium channel inhibition underlies the analgesic effects of the endogenous lipoamino acids. *J Neurosci* **29**(42): 13106-13114.

Basbaum AI, Bautista DM, Scherrer G and Julius D (2009) Cellular and molecular mechanisms of pain. *Cell* **139**(2): 267-284.

Ben-Shabat S, Fride E, Sheskin T, Tamiri T, Rhee MH, Vogel Z, Bisogno T, De Petrocellis L, Di Marzo V and Mechoulam R (1998) An entourage effect: inactive endogenous fatty acid glycerol esters enhance 2-arachidonoyl-glycerol cannabinoid activity. *Eur J Pharmacol* **353**(1): 23-31.

Bisogno T, Melck D, Bobrov M, Gretskaya NM, Bezuglov VV, De Petrocellis L and Di Marzo V (2000) N-acyl-dopamines: novel synthetic CB(1) cannabinoid-receptor ligands and inhibitors of anandamide inactivation with cannabimimetic activity in vitro and in vivo. *Biochem J* **351 Pt 3**: 817-824.

Bisogno T, Melck D, De Petrocellis L, Bobrov M, Gretskaya NM, Bezuglov VV, Sitachitta N, Gerwick WH and Di Marzo V (1998) Arachidonoylserotonin and other novel inhibitors of fatty acid amide hydrolase. *Biochem Biophys Res Commun* **248**(3): 515-522.

Bradshaw HB and Walker JM (2005) The expanding field of cannabimimetic and related lipid mediators. *Br J Pharmacol* **144**(4): 459-465.

Burstein S (2008) The elmiric acids: biologically active anandamide analogs. *Neuropharmacology* **55**(8): 1259-1264.

Cain SM and Snutch TP (2010) Contributions of T-type calcium channel isoforms to neuronal firing. *Channels (Austin)* **4**(6): 475-482.

Downloaded from molpharm.aspetjournals.org at ASPET Journals on April 9, 2024

Chemin J, Monteil A, Perez-Reyes E, Nargeot J and Lory P (2001) Direct inhibition of T-type calcium channels by the endogenous cannabinoid anandamide. *Embo J* **20**(24): 7033-7040.

Chemin J, Nargeot J and Lory P (2007) Chemical determinants involved in anandamide-induced inhibition of T-type calcium channels. *J Biol Chem* **282**(4): 2314-2323.

Chen C and Bazan NG (2005) Lipid signaling: sleep, synaptic plasticity, and neuroprotection. *Prostaglandins Other Lipid Mediat* **77**(1-4): 65-76.

Childers SR, Sexton T and Roy MB (1994) Effects of anandamide on cannabinoid receptors in rat brain membranes. *Biochem Pharmacol* **47**(4): 711-715.

Danthi SJ, Enyeart JA and Enyeart JJ (2005) Modulation of native T-type calcium channels by omega-3 fatty acids. *Biochem Biophys Res Commun* **327**(2): 485-493.

De Petrocellis L, Davis JB and Di Marzo V (2001) Palmitoylethanolamide enhances anandamide stimulation of human vanilloid VR1 receptors. *FEBS Lett* **506**(3): 253-256.

Deutsch DG and Chin SA (1993) Enzymatic synthesis and degradation of anandamide, a cannabinoid receptor agonist. *Biochem Pharmacol* **46**(5): 791-796.

Francois A, Kerckhove N, Meleine M, Alloui A, Barrere C, Gelot A, Uebele VN, Renger JJ, Eschalier A, Ardid D and Bourinet E (2013) State-dependent properties of a new T-type calcium channel blocker enhance Ca(V)3.2 selectivity and support analgesic effects. *Pain* **154**(2): 283-293.

Gilmore AJ, Heblinski M, Reynolds A, Kassiou M and Connor M (2012) Inhibition of human recombinant T-type calcium channels by N-arachidonoyl 5-HT. *Br J Pharmacol* **167**(5): 1076-1088.

Giordanetto F, Knerr L and Wallberg A (2011) T-type calcium channels inhibitors: a patent review. *Expert Opin Ther Pat* **21**(1): 85-101.

Downloaded from molpharm.aspetjournals.org at ASPET Journals on April 9, 2024

Molecular Pharmacology Fast Forward. Published on November 8, 2013 as DOI: 10.1124/mol.113.089581
This article has not been copyedited and formatted. The final version may differ from this version.

Ho WS, Barrett DA and Randall MD (2008) 'Entourage' effects of N-palmitoylethanolamide and N-oleoylethanolamide on vasorelaxation to anandamide occur through TRPV1 receptors. *Br J Pharmacol* **155**(6): 837-846.

Huang SM, Bisogno T, Petros TJ, Chang SY, Zavitsanos PA, Zipkin RE, Sivakumar R, Coop A, Maeda DY, De Petrocellis L, Burstein S, Di Marzo V and Walker JM (2001) Identification of a new class of molecules, the arachidonyl amino acids, and characterization of one member that inhibits pain. *J Biol Chem* **276**(46): 42639-42644.

Kraus RL, Li Y, Gregan Y, Gotter AL, Uebele VN, Fox SV, Doran SM, Barrow JC, Yang ZQ, Reger TS, Koblan KS and Renger JJ (2010) In vitro characterization of T-type calcium channel antagonist TTA-A2 and in vivo effects on arousal in mice. *J Pharmacol Exp Ther* **335**(2): 409-417.

Kuo IY, Wolfle SE and Hill CE (2011) T-type calcium channels and vascular function: the new kid on the block? *J Physiol* **589**(Pt 4): 783-795.

Leaf A, Xiao YF, Kang JX and Billman GE (2003) Prevention of sudden cardiac death by n-3 polyunsaturated fatty acids. *Pharmacol Ther* **98**(3): 355-377.

Lee J and Shin HS (2007) T-type calcium channels and thalamocortical rhythms in sleep: a perspective from studies of T-type calcium channel knockout mice. *CNS Neurol Disord Drug Targets* **6**(1): 63-69.

Lory P, Bidaud I and Chemin J (2006) T-type calcium channels in differentiation and proliferation. *Cell Calcium* **40**(2): 135-146.

Lory P and Chemin J (2007) Towards the discovery of novel T-type calcium channel blockers. *Expert Opin Ther Targets* **11**(5): 717-722.

Martin RL, Lee JH, Cribbs LL, Perez-Reyes E and Hanck DA (2000) Mibefradil block of cloned T-type calcium channels. *J Pharmacol Exp Ther* **295**(1): 302-308.

Downloaded from molpharm.aspetjournals.org at ASPET Journals on April 9, 2024

McGivern JG (2006) Pharmacology and drug discovery for T-type calcium channels. *CNS Neurol Disord Drug Targets* **5**(6): 587-603.

Ono K and Iijima T (2010) Cardiac T-type Ca^{2+} channels in the heart. *J Mol Cell Cardiol* **48**(1): 65-70.

Perez-Reyes E (2003) Molecular physiology of low-voltage-activated t-type calcium channels. *Physiol Rev* **83**(1): 117-161.

Pinto JC, Potie F, Rice KC, Boring D, Johnson MR, Evans DM, Wilken GH, Cantrell CH and Howlett AC (1994) Cannabinoid receptor binding and agonist activity of amides and esters of arachidonic acid. *Mol Pharmacol* **46**(3): 516-522.

Reger TS, Yang ZQ, Schlegel KA, Shu Y, Mattern C, Cube R, Rittle KE, McGaughey GB, Hartman GD, Tang C, Ballard J, Kuo Y, Prueksaritanont T, Nuss CE, Doran SM, Fox SV, Garson SL, Li Y, Kraus RL, Uebele VN, Renger JJ and Barrow JC (2011) Pyridyl amides as potent inhibitors of T-type calcium channels. *Bioorg Med Chem Lett* **21**(6): 1692-1696.

Roman RJ (2002) P-450 metabolites of arachidonic acid in the control of cardiovascular function. *Physiol Rev* **82**(1): 131-185.

Ross HR, Gilmore AJ and Connor M (2009) Inhibition of human recombinant T-type calcium channels by the endocannabinoid N-arachidonoyl dopamine. *Br J Pharmacol* **156**(5): 740-750.

Saghatelian A, McKinney MK, Bandell M, Patapoutian A and Cravatt BF (2006) A FAAH-regulated class of N-acyl taurines that activates TRP ion channels. *Biochemistry* **45**(30): 9007-9015.

Saghatelian A, Trauger SA, Want EJ, Hawkins EG, Siuzdak G and Cravatt BF (2004) Assignment of endogenous substrates to enzymes by global metabolite profiling. *Biochemistry* **43**(45): 14332-14339.

Downloaded from molpharm.aspetjournals.org at ASPET Journals on April 9, 2024

Molecular Pharmacology Fast Forward. Published on November 8, 2013 as DOI: 10.1124/mol.113.089581
This article has not been copyedited and formatted. The final version may differ from this version.

Santi CM, Cayabyab FS, Sutton KG, McRory JE, Mezeyova J, Hamming KS, Parker D, Stea A and Snutch TP (2002) Differential inhibition of T-type calcium channels by neuroleptics. *J Neurosci* **22**(2): 396-403.

Talavera K, Staes M, Janssens A, Droogmans G and Nilius B (2004) Mechanism of arachidonic acid modulation of the T-type Ca^{2+} channel alpha1G. *J Gen Physiol* **124**(3): 225-238.

Todorovic SM and Jevtovic-Todorovic V (2013) Neuropathic pain: role for presynaptic T-type channels in nociceptive signaling. *Pflugers Arch* **465**(7): 921-927.

Uebele VN, Gotter AL, Nuss CE, Kraus RL, Doran SM, Garson SL, Reiss DR, Li Y, Barrow JC, Reger TS, Yang ZQ, Ballard JE, Tang C, Metzger JM, Wang SP, Koblan KS and Renger JJ (2009a) Antagonism of T-type calcium channels inhibits high-fat diet-induced weight gain in mice. *J Clin Invest* **119**(6): 1659-1667.

Uebele VN, Nuss CE, Fox SV, Garson SL, Cristescu R, Doran SM, Kraus RL, Santarelli VP, Li Y, Barrow JC, Yang ZQ, Schlegel KA, Rittle KE, Reger TS, Bednar RA, Lemaire W, Mullen FA, Ballard JE, Tang C, Dai G, McManus OB, Koblan KS and Renger JJ (2009b) Positive allosteric interaction of structurally diverse T-type calcium channel antagonists. *Cell Biochem Biophys* **55**(2): 81-93.

Uslaner JM, Smith SM, Huszar SL, Pachmerhiwala R, Hinchliffe RM, Vardigan JD, Nguyen SJ, Surles NO, Yao L, Barrow JC, Uebele VN, Renger JJ, Clark J and Hutson PH (2012) T-type calcium channel antagonism produces antipsychotic-like effects and reduces stimulant-induced glutamate release in the nucleus accumbens of rats. *Neuropharmacology* **62**(3): 1413-1421.

Uslaner JM, Vardigan JD, Drott JM, Uebele VN, Renger JJ, Lee A, Li Z, Le AD and Hutson PH (2010) T-type calcium channel antagonism decreases motivation for nicotine and

Downloaded from molpharm.aspetjournals.org at ASPET Journals on April 9, 2024

Molecular Pharmacology Fast Forward. Published on November 8, 2013 as DOI: 10.1124/mol.113.089581
This article has not been copyedited and formatted. The final version may differ from this version.

blocks nicotine- and cue-induced reinstatement for a response previously reinforced with nicotine. *Biol Psychiatry* **68**(8): 712-718.

Weiss N and Zamponi GW (2012) Control of low-threshold exocytosis by T-type calcium channels. *Biochim Biophys Acta*.

Xie X, Van Deusen AL, Vitko I, Babu DA, Davies LA, Huynh N, Cheng H, Yang N, Barrett PQ and Perez-Reyes E (2007) Validation of high throughput screening assays against three subtypes of Ca(v)3 T-type channels using molecular and pharmacologic approaches. *Assay Drug Dev Technol* **5**(2): 191-203.

Zhang Y, Cribbs LL and Satin J (2000) Arachidonic acid modulation of alpha1H, a cloned human T-type calcium channel. *Am J Physiol Heart Circ Physiol* **278**(1): H184-193.

Downloaded from molpharm.aspetjournals.org at ASPET Journals on April 9, 2024

Molecular Pharmacology Fast Forward. Published on November 8, 2013 as DOI: 10.1124/mol.113.089581
This article has not been copyedited and formatted. The final version may differ from this version.

Footnotes

This work was supported by the French Ministry of Research Agence Nationale pour la Recherche [Grant ANR-09-MNPS-035].

Reprint Requests should be addressed to Dr. Jean Chemin, Institut de Génomique Fonctionnelle, Universités Montpellier 1 & 2, Centre National de la Recherche Scientifique (CNRS), Unité Mixte de Recherche (UMR) 5203, INSERM U661, LabEx 'Ion Channel Science and Therapeutics', 141, rue de la Cardonille, 34094 Montpellier cedex 05, France.

Phone: +33 4 34 35 92 50 / Fax: +33 4 67 54 24 32 / Email : jean.chemin@igf.cnrs.fr

Downloaded from molpharm.aspetjournals.org at ASPET Journals on April 9, 2024

Molecular Pharmacology Fast Forward. Published on November 8, 2013 as DOI: 10.1124/mol.113.089581
This article has not been copyedited and formatted. The final version may differ from this version.

Figure Legends.

Figure 1.

Inhibition of $Ca_v3.3$ currents by endogenous lipids. (**A-B**) Inhibition of $Ca_v3.3$ currents by 3 µM *N*-docosahexaenoyl glycine (22:6 Gly) and subsequent washout with a solution containing 3 mg/ml BSA. $Ca_v3.3$ currents were elicited by a 450 ms depolarization to -30 mV from a holding potential (HP) of -75 mV (A) or -110 mV (B) at a frequency of 0.2 Hz. (**C**) Time course of the decrease in $Ca_v3.3$ current amplitude during 22:6 Gly application at HP -75 mV and subsequent washout with the BSA solution. Same cell than in (A). (**D**) Inhibition of $Ca_v3.3$ currents by *N*-arachidoyl glycine (20:0 Gly) at HP -75 mV and subsequent washout with a solution containing 3 mg/ml BSA. (**E**) Summary of the inhibitory effect on $Ca_v3.3$ current at HP -75 mV of 20:0 Gly, 18:2 Gly (*N*-linoleoyl glycine), 20:4 Gly (*N*-arachidonoyl glycine, *N*AGly), 22:6 Gly, *N*-arachidonoyl-3-OH-γ-butyric acid (*N*AGABA-OH), *N*-arachidonoyl-γ-butyric acid (*N*AGABA), *N*-arachidonoyl-L-serine (*N*ASer), *N*-arachidonoyl alanine (*N*AAla), *N*-arachidonoyl ethanolamine (anandamide, *N*AEA), *N*-arachidonoyl taurine (*N*ATau), *N*-arachidonoyl serotonin (*N*A-5HT) and *N*-arachidonoyl dopamine (*N*ADA).

Figure 2.

Effects of *N*AGly on biophysical properties of $Ca_v3.3$ currents. **(A)** Current-voltage (I-V) curves of $Ca_v3.3$ current in the absence and in the presence of 1 µM and 3 µM *N*AGly. Currents were elicited by increasing depolarizations (-80 to +10 mV) from a HP of -80 mV at a frequency of 0.2 Hz. (**B-C**). Effects of 1 and 3 µM *N*AGly on inactivation (τ_{inac}, B) and activation (τ_{act}, C) kinetics of $Ca_v3.3$ currents. (**D**) Steady-state inactivation curves of $Ca_v3.3$ currents in the absence and in the presence of 1 µM and 3 µM *N*AGly. Currents were recorded at -30 mV from HPs ranging from -110 to -50 mV (5 s duration). (**E**) Recovery from inactivation of $Ca_v3.3$ current in the absence and in the presence of 1 µM and 3 µM *N*AGly.

Downloaded from molpharm.aspetjournals.org at ASPET Journals on April 9, 2024

Molecular Pharmacology Fast Forward. Published on November 8, 2013 as DOI: 10.1124/mol.113.089581
This article has not been copyedited and formatted. The final version may differ from this version.

Recovery from inactivation was measured using two -30 mV depolarizations lasting 450 ms, which were applied from a HP of -80 mV of increasing duration. (**F**) Effects of 1 and 3 µM *N*AGly on deactivation kinetics of $Ca_v3.3$ currents (τ_{deac}). Currents were elicited by a 28 ms depolarization at -30 mV and deactivation kinetics were measured at repolarization potentials ranging from -130 to -60 mV.

Figure 3.

Inhibition of $Ca_v3.3$ currents by combined application of endogenous lipids and TTA-A2. (**A**) Effect of a 300 nM *N*AEA solution (2) followed by the application of both 300 nM *N*AEA and 3 nM TTA-A2 (3), compared to the control solution (1). (**B**) Effect of a 3 nM TTA-A2 solution followed by the application of both 300 nM *N*AEA and 3 nM TTA-A2. (**C**) Effect of a solution containing both 300 nM *N*AEA and 3 nM TTA-A2. (**D-F**) Similar experiments with 3 µM *N*A-5HT and 3 nM TTA-A2. (**G**) Summary of the average effects of *N*AEA, *N*ADA and *N*A-5HT alone or combined with 3 nM TTA-A2. Currents were elicited at -30 mV from a HP of -75 mV at a frequency of 0.2 Hz. *, $p<0.05$; **, $p<0.01$; ***, $p<0.001$; *n.s.*, non significant.

Figure 4.

Displacement of $[^3H]$ TTA-A1 binding by *N*-acyl amino acids (**A**), by *N*-acyl ethanolamines (**B**) and *N*-acyl neurotransmitters (**C**). Lipids are *N*-arachidonoyl-L-serine (*N*ASer), *N*-arachidonoyl glycine (*N*AGly), *N*-arachidoyl glycine (20:0 Gly), *N*-arachidonoyl ethanolamine (*N*AEA, 20:4), *N*-arachidoyl ethanolamine (20:0 EA), *N*-arachidonoyl dopamine (*N*ADA, 20:4), *N*-arachidonoyl serotonin (*N*A-5HT, 20:4) and *N*-arachidonoyl taurine (*N*ATau, 20:4).

Downloaded from molpharm.aspetjournals.org at ASPET Journals on April 9, 2024

Molecular Pharmacology Fast Forward. Published on November 8, 2013 as DOI: 10.1124/mol.113.089581
This article has not been copyedited and formatted. The final version may differ from this version.

Figure 5.

Inhibition of $Ca_v3.3$ currents by combined application of endogenous lipids and TTA-Q4. (**A**) Effect of a 20 nM TTA-Q4 solution followed by the application of both 100 nM *N*AEA and a 20 nM TTA-Q4. (**B**) Effect of a 100 nM *N*AEA solution followed by the application of both 100 nM *N*AEA and 20 nM TTA-Q4. (**C**) Effect of a solution containing both 100 nM *N*AEA and a 20 nM TTA-Q4. (**D**) Time course of the decrease in $Ca_v3.3$ current amplitude during application of 100 nM *N*AEA and 20 nM TTA-Q4. Same cell than in (C). (**E-H**) Similar experiments with 20 nM TTA-Q4 and 300 nM *N*A-5HT. (**I**) Summary of the effects of *N*AEA, *N*ADA and *N*A-5HT alone or combined with 20 nM TTA-Q4. The arrows indicate the anticipated sum of the effects of lipids plus TTA-Q4. Currents were elicited at -30 mV from a HP of -75 mV at a frequency of 0.2 Hz. *, $p<0.05$; ***, $p<0.001$; *n.s.*, non significant.

Downloaded from molpharm.aspetjournals.org at ASPET Journals on April 9, 2024

Molecular Pharmacology Fast Forward. Published on November 8, 2013 as DOI: 10.1124/mol.113.089581
This article has not been copyedited and formatted. The final version may differ from this version.

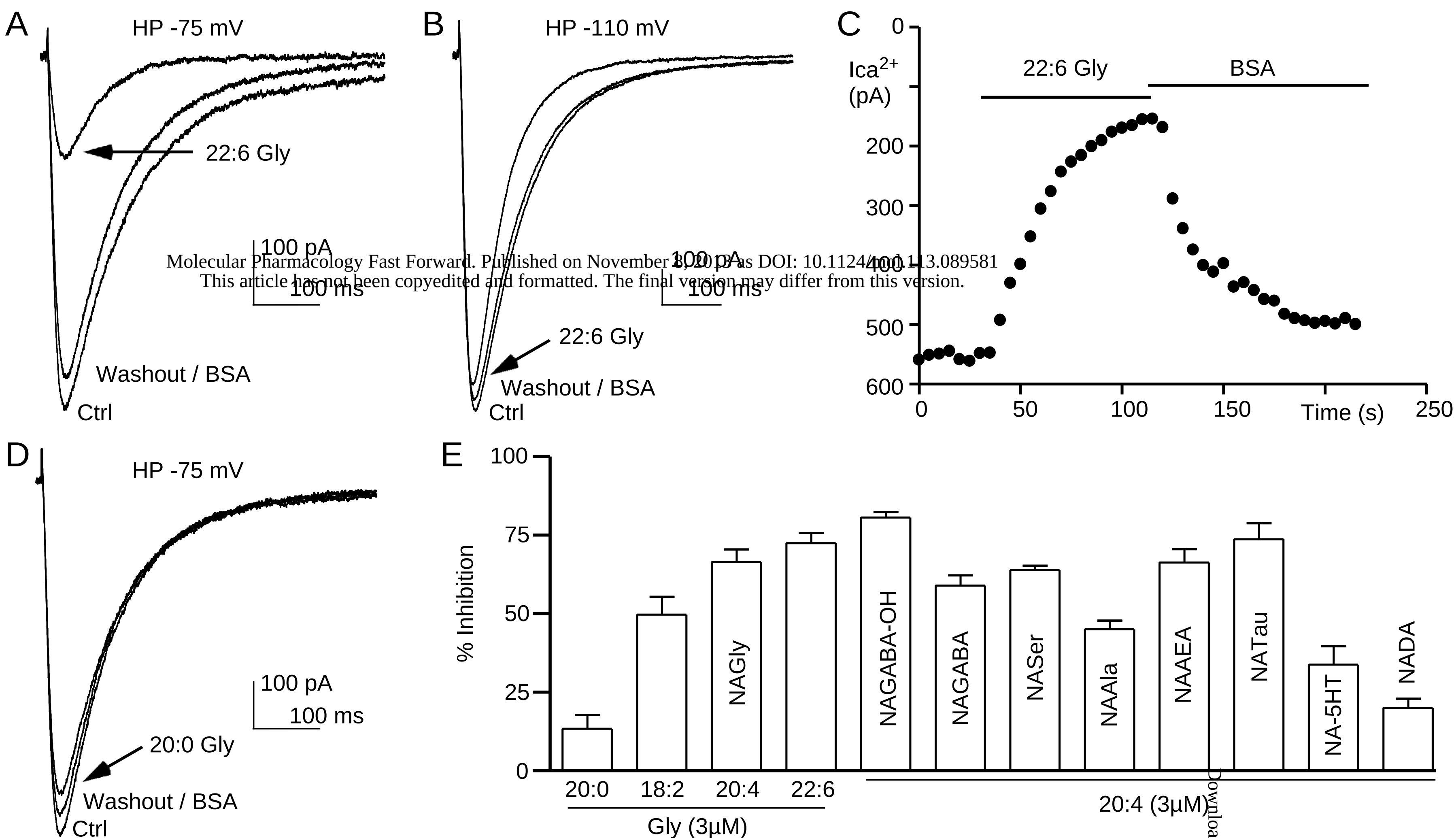

Figure 1

Downloaded from molpharm.aspetjournals.org at ASPET Journals on April 9, 2024

Molecular Pharmacology Fast Forward. Published on November 8, 2013 as DOI: 10.1124/mol.113.089581
This article has not been copyedited and formatted. The final version may differ from this version.

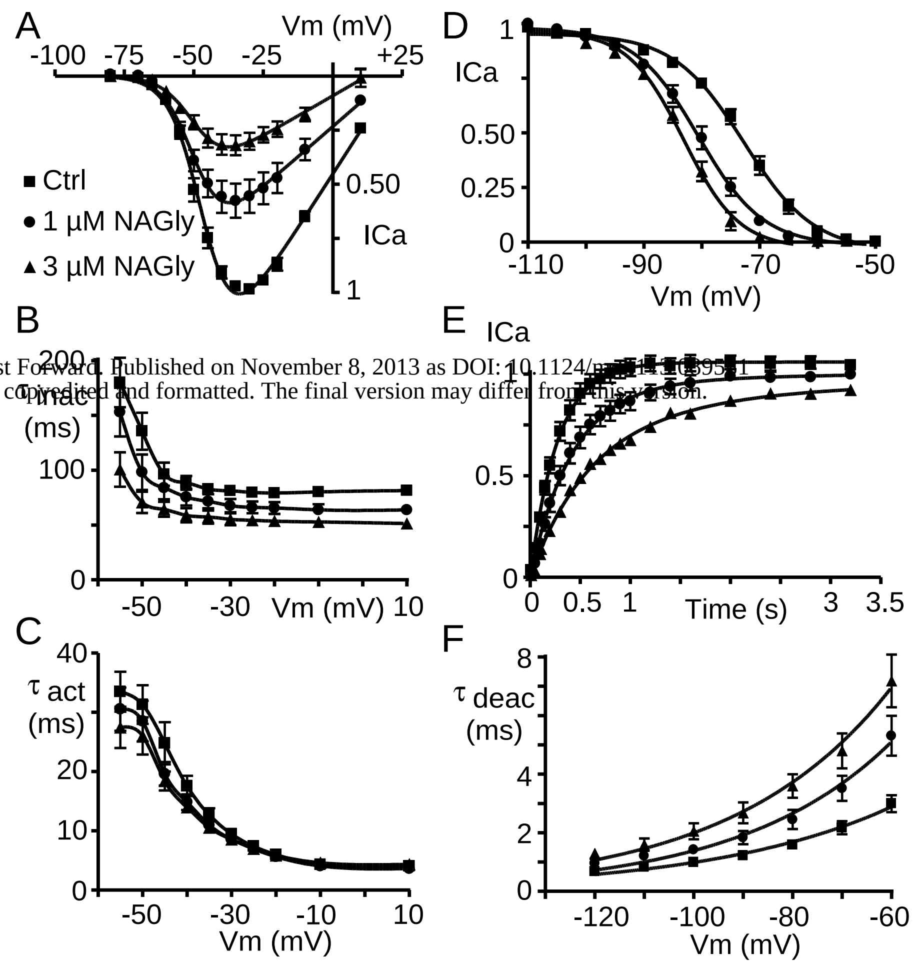

Figure 2

Downloaded from molpharm.aspetjournals.org at ASPET Journals on April 9, 2024

Molecular Pharmacology Fast Forward. Published on November 8, 2013 as DOI: 10.1124/mol.113.089581
This article has not been copyedited and formatted. The final version may differ from this version.

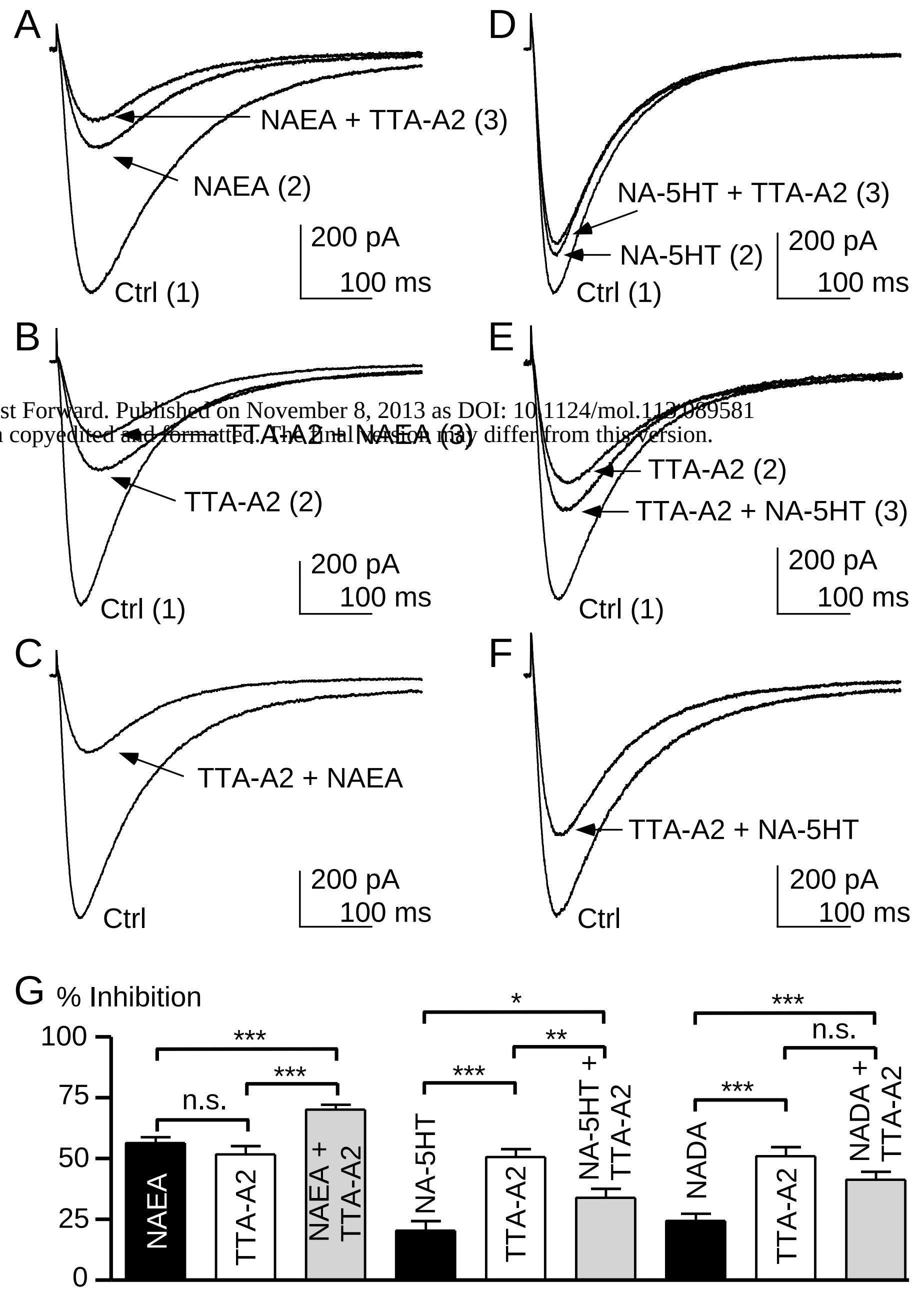

Figure 3

Downloaded from molpharm.aspetjournals.org at ASPET Journals on April 9, 2024

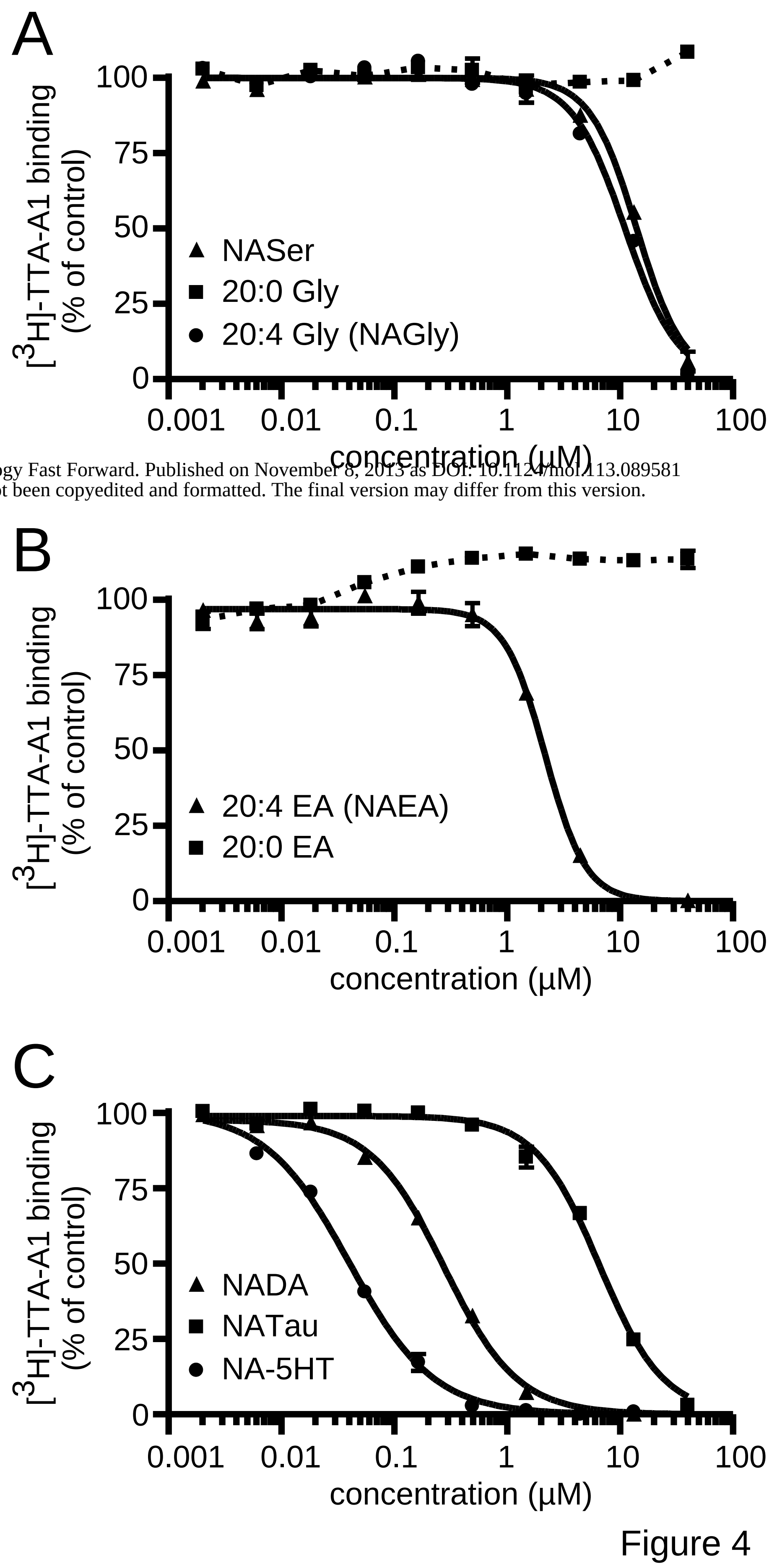

Figure 4

Molecular Pharmacology Fast Forward. Published on November 8, 2013 as DOI: 10.1124/mol.113.089581
This article has not been copyedited and formatted. The final version may differ from this version.

Downloaded from molpharm.aspetjournals.org at ASPET Journals on April 9, 2024

Molecular Pharmacology Fast Forward. Published on November 8, 2013 as DOI: 10.1124/mol.113.089581
This article has not been copyedited and formatted. The final version may differ from this version.

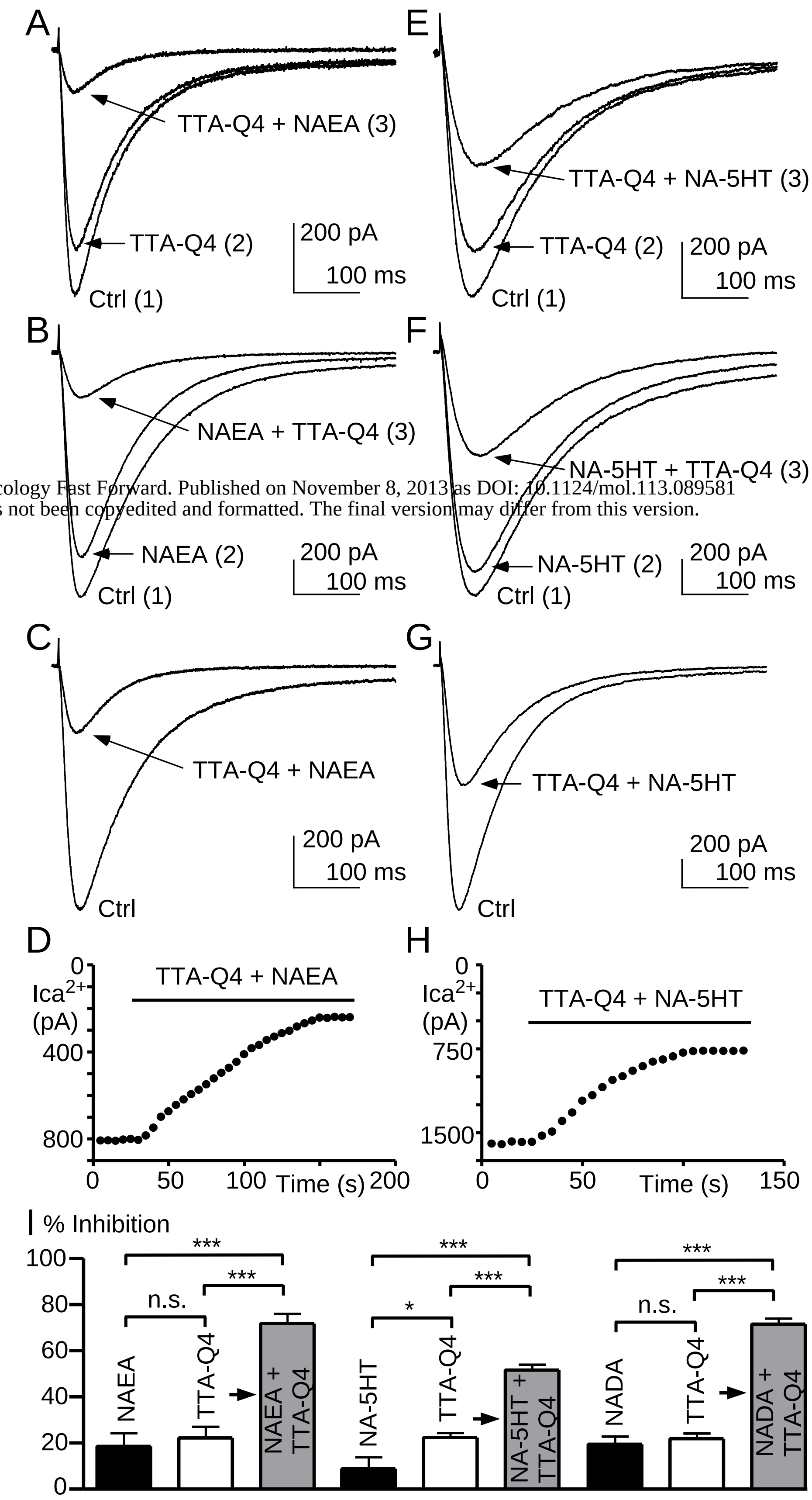

Figure 5

Downloaded from molpharm.aspetjournals.org at ASPET Journals on April 9, 2024